

## A (2 + 1)-flavor lattice study of the pion quasiparticle in the thermal hadronic phase at physical quark masses

Ardit Krasniqi,<sup>a,\*</sup> Marco Cè,<sup>b</sup> Tim Harris,<sup>c</sup> Harvey B. Meyer,<sup>a,d,e</sup> Csaba Török<sup>a</sup> and Samuel Ruhl<sup>a</sup>

<sup>a</sup>PRISMA<sup>+</sup> Cluster of Excellence & Institut für Kernphysik, Johannes Gutenberg-Universität Mainz, D-55099 Mainz, Germany

<sup>b</sup>Albert Einstein Center for Fundamental Physics (AEC) and Institut für Theoretische Physik, Universität Bern, Sidlerstrasse 5, CH-3012 Bern, Switzerland

<sup>c</sup>School of Physics and Astronomy, University of Edinburgh, EH9 3JZ, UK

<sup>d</sup>Helmholtz Institut Mainz, Johannes Gutenberg-Universität Mainz, D-55099 Mainz, Germany

<sup>e</sup>GSI Helmholtzzentrum für Schwerionenforschung, Darmstadt, Germany

E-mail: [arkrasni@uni-mainz.de](mailto:arkrasni@uni-mainz.de)

**Abstract.** We investigate the properties of the pion quasiparticle in the thermal hadronic phase of (2 + 1)-flavor QCD on the lattice at physical quark masses at a temperature  $T = 128$  MeV. We find that the pion quasiparticle mass  $\omega_0 = 113(3)$  MeV is significantly reduced relative to the zero-temperature pion mass  $m_\pi^0 = 128(1)$  MeV, by contrast with the static screening mass  $m_\pi = 144(3)$  MeV, which increases with temperature. On the other hand the pion quasiparticle decay constant does not change much compared to the corresponding zero-temperature decay constant. The difference of the vector- and axialvector spectral functions serves as an order parameter of chiral symmetry restoration. By analyzing this quantity we conclude that chiral symmetry restoration is already at an advanced stage in the spectral function.

*The 39th International Symposium on Lattice Field Theory,  
8th-13th August, 2022,  
Rheinische Friedrich-Wilhelms-Universität Bonn, Bonn, Germany*

---

\*Speaker

**Table 1:** Parameters and lattice spacing of the ensemble analyzed in this paper. The lattice spacing determination is from Ref. [8].

$\beta/a$	$L/a$	$6/g_0^2$	$\kappa_l$	$\kappa_s$	$a$ [fm]
24	96	3.55	0.137232867	0.136536633	0.06426(76)

## 1. Introduction

In the early universe the strongly interacting constituents, namely weakly coupled quarks and gluons, were in a hot and dense phase which we now call *Quark-Gluon Plasma* (QGP). In this phase no individual color charges can be assigned to a hadron due to color screening. However, as a consequence of the continuous expansion, the universe has gradually cooled down. Finally – at a certain temperature  $T_c$  – a phase transition to the confined hadronic phase occurred.

In order to estimate the bulk properties of the hadronic phase with increasing temperature, often the *hadron resonance gas* (HRG) model is employed [1]. It describes the thermodynamic properties of the system by the sum of partial contributions of non-interacting hadron species up to a certain cut-off mass.

Here we extend previous 2-flavor studies on the pion quasiparticle [2, 3] to the (2+1)-flavor case on an ensemble with physical quark masses. We present a modified dispersion relation for the pion quasiparticle and use it to estimate the *quark number susceptibility* (QNS) on our ensemble. Furthermore, we examine the Dey-Eleetsky-Ioffe mixing theorem at finite quark mass [4–6].

In these proceedings we show the results presented at the Lattice conference in August 2022. Updated results, together with a more detailed study of the pion quasiparticle and an investigation of several aspects of chiral symmetry at a temperature  $T = 128$  MeV, are available in our recent preprint [7].

## 2. Numerical setup

Our calculations are performed on an  $N_f = 2 + 1$  ensemble with tree-level  $O(a^2)$ -improved Lüscher-Weisz gauge action and non-perturbatively  $O(a)$ -improved Wilson fermions [9]. The ensemble has been generated using version 2.0 of the openQCD package see, Ref. [10].

We employ a single gauge ensemble of size  $24 \times 96^3$  of  $O(a)$ -improved Wilson fermions with physical quark masses at a temperature

$$T = \frac{1}{\beta} = \frac{1}{24a} = 127.9(1.5) \text{ MeV}. \quad (1)$$

The physical and algorithmic parameters are listed in Tab. (1). There exists a corresponding zero-temperature *Coordinated Lattice Simulations* (CLS) [11] ensemble with identical parameters apart from its time extent. For reference we quote the pion mass and the decay constant of this ensemble determined in Ref. [12],

$$T = 0 : \quad m_\pi^0 = 128.1(1.3)(1.5) \text{ MeV}, \quad f_\pi^0 = 87.4(0.4)(1.0) \text{ MeV}, \quad (2)$$

where the first error is from the corresponding quantity in lattice units, and the second is from the lattice spacing determination of Ref. [8].

### 3. Preliminaries

#### 3.1 Basic definitions

We define the pseudoscalar density, the vector current and the axial- vector current as

$$P^a(x) = \bar{\psi}(x)\gamma_5\frac{\tau^a}{2}\psi(x), \quad V_\mu^a(x) = \bar{\psi}(x)\gamma_\mu\frac{\tau^a}{2}\psi(x), \quad A_\mu^a(x) = \bar{\psi}(x)\gamma_\mu\gamma_5\frac{\tau^a}{2}\psi(x), \quad (3)$$

where  $a \in \{1, 2, 3\}$  is an adjoint  $SU(2)_{\text{isospin}}$  index,  $\tau^a$  is a Pauli matrix and  $\psi(x)$  is a Dirac field flavor doublet. With the aid of the *partially conserved axial current* (PCAC)-relation

$$\partial_\mu A_\mu^a(x) = 2m_{\text{PCAC}}P^a(x), \quad (4)$$

one can relate the screening pseudoscalar correlator to the screening axial correlator projected to zero spatial momentum,

$$G_P^s(x_3, T, \mathbf{p} = 0) = -\frac{1}{4m_{\text{PCAC}}^2} \frac{\partial^2}{\partial x_3^2} G_A^s(x_3, T, \mathbf{p} = 0). \quad (5)$$

The asymptotic form of the static screening axial correlator,

$$\delta^{ab} G_A^s(x_3, T, \mathbf{p} = 0) = \int dx_0 d^2x_\perp \langle A_3^{a,\text{imp}}(x) A_3^{b,\text{imp}}(0) \rangle \stackrel{x_3 \rightarrow \infty}{\approx} \delta^{ab} \frac{f_\pi^2 m_\pi}{2} e^{-m_\pi x_3}, \quad (6)$$

defines the screening pion mass  $m_\pi$  and the screening decay constant  $f_\pi$ .

#### 3.2 Pion velocity and modified dispersion relation

In Refs. [13, 14] Son and Stephanov have shown that

$$\omega_{\mathbf{p}} = u(T) \sqrt{m_\pi^2 + \mathbf{p}^2}, \quad \text{for any } T \lesssim T_C \quad (7)$$

describes the real part of the dispersion relation of a pion quasiparticle in the low-temperature phase of QCD. The temperature-dependent parameter  $u$  indicates that the thermal medium breaks Lorentz invariance and is accessible from lattice calculations. Under the assumption that the pion dominates the Euclidean two-point functions of the axial current time component  $A_0$  and of the pseudoscalar density  $P$ , two estimators

$$u_m = \left[ -\frac{4m_q^2}{m_\pi^2} \frac{G_P(x_0, T, \mathbf{p} = 0)}{G_A(x_0, T, \mathbf{p} = 0)} \Big|_{x_0=\beta/2} \right]^{1/2}, \quad (8)$$

$$u_f = \frac{f_\pi^2 m_\pi}{2G_A(\beta/2, T, \mathbf{p} = 0) \sinh(u_f m_\pi \beta/2)}, \quad (9)$$

for the pion velocity can be obtained [2, 3].

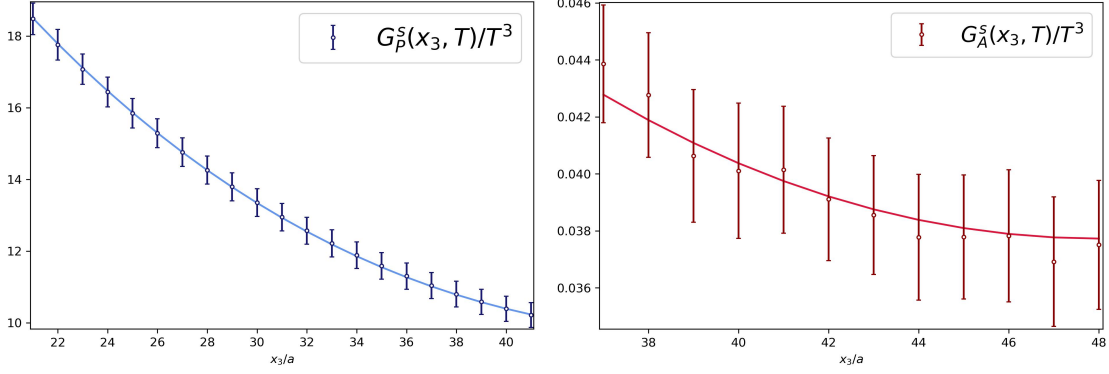


**Figure 1:** **Left panel:** Renormalized screening correlation function  $G_P^s(x_3, T)/T^3$  and the result of the fit. The chosen fit interval is  $x_3/a \in [21, 41]$ . **Right panel:** Renormalized screening correlation function  $G_A^s(x_3, T)/T^3$  and the result of the fit with a prior from  $G_P^s(x_3, T)$ . The chosen fit interval in this case is  $x_3/a \in [37, 48]$ .

## 4. Results

### 4.1 Pion quantities at finite temperature

Making use of the PCAC-based relation (5), a one-state fit ansatz for the corresponding correlation functions can be formulated in the form

$$G_A^s(x_3, T, \mathbf{p} = 0) = \frac{A_1^2 m_1}{2} \cosh[(m_1(x_3 - L/2))], \quad (10)$$

$$G_P^s(x_3, T, \mathbf{p} = 0) = -\frac{A_1^2 m_1^3}{8m_{\text{PCAC}}^2} \cosh[(m_1(x_3 - L/2))]. \quad (11)$$

The results of the correlated fits are shown in Fig. 1. Exploiting the better signal-to-noise ratio the screening pion mass  $m_\pi$  was first extracted using the pseudoscalar correlator  $G_P^s$ . Next, the axial correlator  $G_A^s$  has been fitted using the fit parameters obtained from  $G_P^s$  as a prior. Making use of Eq. (6) the screening decay constant  $f_\pi$  can be extracted in terms of the fit parameter  $A_1$  via

$$f_\pi = A_1 \sqrt{\sinh(m_1 L/2)}. \quad (12)$$

The corresponding quasiparticle quantities can be obtained using the estimator  $u_m$  and the results are listed in Table 2. At finite temperature we observe a ‘splitting’ into a higher screening pion mass  $m_\pi = 144(3)$  MeV and a lower quasiparticle mass  $\omega_0 = 113(3)$  MeV, relative to the zero-temperature pion mass  $m_\pi^0 = 128(1)$  MeV [see Eq. (2)]. The screening pion decay constant  $f_\pi = 72(1)$  MeV behaves in the opposite way and is 17% lower than the zero-temperature pion decay constant  $f_\pi^0 = 87(1)$  MeV.<sup>1</sup> However, the quasiparticle decay constant  $f_\pi^t = f_\pi/u_m = 91(2)$  MeV is certainly no smaller than  $f_\pi^0$ . We also find that the two estimators  $u_f$  and  $u_m$  of the pion velocity agree very well and additionally differ significantly from unity, indicating a clear breaking of Lorentz boost invariance.

**Table 2:** Summary of the results of the E250 thermal ensemble with  $N_\tau = 24$ . The pion quasiparticle mass  $\omega_0$  is calculated using  $\omega_0 = u_m m_\pi$  and the quasiparticle decay constant  $f_\pi^t$  is obtained using  $f_\pi^t = f_\pi/u_m$ . Note that in Ref. [7] we obtained a slightly more precise value for the pion decay constant including the  $PA_0$ -correlator.

$m_\pi/T$	1.121(21)
$f_\pi/T$	0.558(14)
$u_f$	0.787(16)
$u_m$	0.786(18)
$u_f/u_m$	1.001(27)
$\omega_0/T$	0.881(23)
$f_\pi^t/T$	0.710(19)

## 4.2 Dey-Elefsky-Ioffe mixing theorem at finite quark mass

In the chiral limit at temperatures well below the chiral phase transition, the heat bath is dominated by massless pions. Using PCAC current algebra, Dey, Elefsky and Ioffe have shown that to order  $T^2$  the vector and axial-vector spectral functions can be obtained from their vacuum equivalents [4–6],

$$\rho_V(\omega, \mathbf{p}, T) = (1 - \epsilon)\rho_V(\omega, \mathbf{p}, T = 0) + \epsilon\rho_A(\omega, \mathbf{p}, T = 0), \quad (13)$$

$$\rho_A(\omega, \mathbf{p}, T) = (1 - \epsilon)\rho_A(\omega, \mathbf{p}, T = 0) + \epsilon\rho_V(\omega, \mathbf{p}, T = 0), \quad (14)$$

where  $\epsilon \equiv T^2/(6(f_\pi^0)^2)$  is a temperature dependent coefficient. As an immediate consequence, the difference of the two spectral functions is proportional to the zero-temperature equivalent,

$$\rho_V(\omega, \mathbf{p}, T) - \rho_A(\omega, \mathbf{p}, T) = (1 - 2\epsilon) [\rho_V(\omega, \mathbf{p}, T = 0) - \rho_A(\omega, \mathbf{p}, T = 0)], \quad (15)$$

with the proportionality factor given by  $(1 - 2\epsilon)$ . Thus, this quantity serves as an order parameter for chiral symmetry restoration and should be investigated even for non-zero quark mass. Therefore, we have analysed the ratio of the difference  $(V - A)$  of the corresponding temporal thermal correlators and the difference  $(V - A)_{\text{rec}}$  of the reconstructed temporal correlators at vanishing spatial momentum. The reconstructed correlator is defined as the thermal correlator that would be realized if the spectral function would not change when the temperature is switched on [15],

$$G_J^{\text{rec}}(x_0, T, \mathbf{p}) = \sum_{m \in \mathbb{Z}} G_J(x_0 + m\beta, 0, \mathbf{p}) \quad (J \in \{V, A\}). \quad (16)$$

As can be seen from Fig. 2, the difference ‘ $V - A$ ’ shows a significant reduction by a factor of  $\approx 0.67$ . Consequently, the spectral function must have changed during the transition from  $T = 0$  to  $T = 128$  MeV. Hence, chiral symmetry restoration is already at an advanced stage in the spectral function. Due to Eq. (15) we would expect the ratio to be flat. In the lattice data, we do observe a flat behaviour of the ratio in the interval  $\beta/4 \leq x_0 \leq 3\beta/4$ .

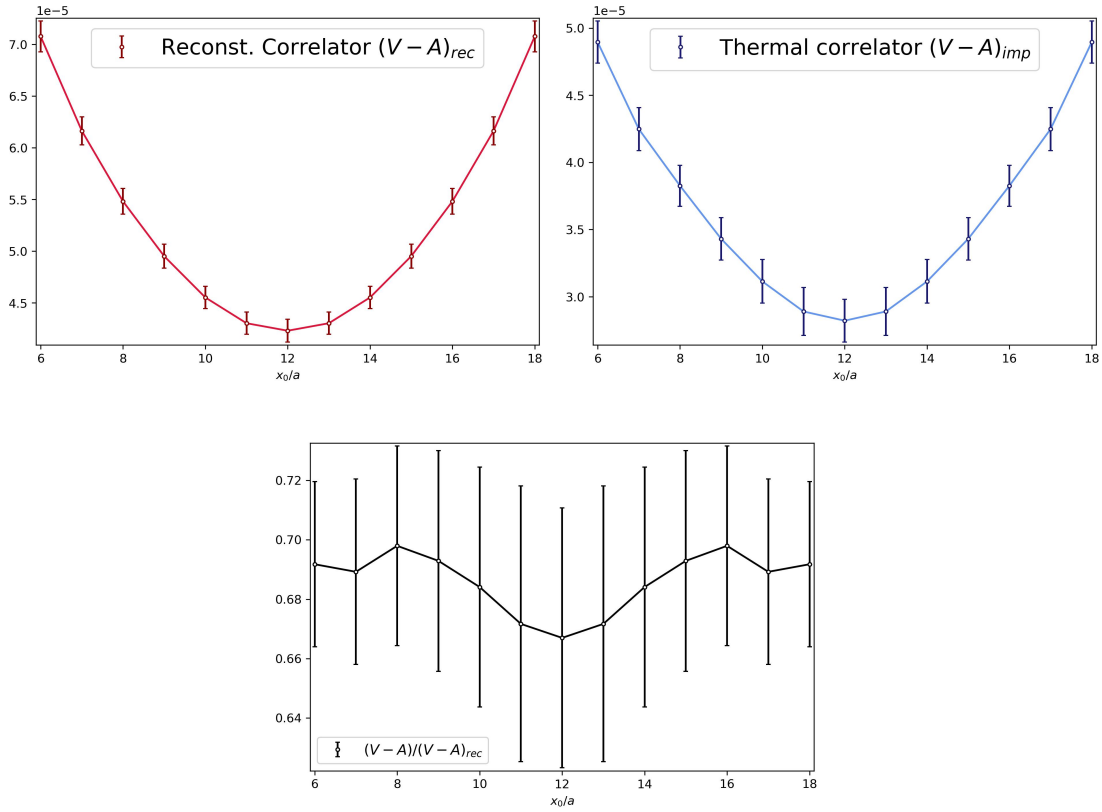


**Figure 2:** Left panel: The reconstructed correlator for the difference ‘ $V - A$ ’. Right panel: The difference of ‘ $V - A$ ’ at  $T \approx 128$  MeV. All renormalization factors are included. Bottom panel: Ratio of the difference ‘ $V - A$ ’ and the difference of the reconstructed correlator ‘ $(V - A)_{rec}$ ’

### 4.3 Quark number susceptibility (QNS)

On the lattice, we define the quark number susceptibility as

$$\chi_q(x_0, T) = Z_V^2(g_0^2) \beta \int d^3x \langle V_0^a(x_0, \mathbf{x}) V_0^a(0, \mathbf{0}) \rangle, \quad x_0 \neq 0, \quad (17)$$

where  $Z_V(g_0^2)$  is a non-perturbatively determined renormalization factor [16].

The result is shown in Fig. (3). As expected the  $(V_0 - V_0)$ -correlator is very flat and the value  $\chi_q(T)/T^2 = 0.2293(47)$  has been determined using a correlated fit to the plateau. The QNS can also be estimated using the hadron resonance gas model, where it is given as the sum

$$(\chi_q)_m. + (\chi_q)_b. \quad (18)$$

with

$$\frac{(\chi_q)_{m./b.}}{T^2} = \frac{2\beta^3}{3} \sum_{\text{multiplets}} (2J+1)I(I+1)(2I+1) \int \frac{d^3\mathbf{p}}{(2\pi)^3} f_{\mathbf{p}}^{B/F} (1 + f_{\mathbf{p}}^{B/F}), \quad (19)$$

being the mesonic and baryonic contribution, respectively. The summation includes all multiplets of spin  $J$  and isospin  $I$  and  $f_{\mathbf{p}}^{B/F} = 1/[e^{\beta\omega_{\mathbf{p}}} \mp 1]$  denote the Bose-Einstein and Fermi-Dirac

<sup>1</sup>Note that in this work the pion decay constant differs by a factor of  $\sqrt{2}$ .

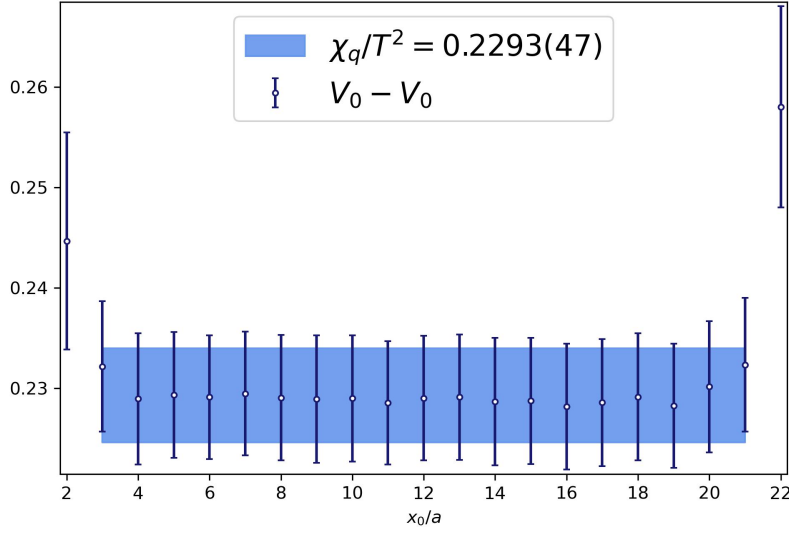


**Figure 3:** Quark number susceptibility extracted from the local vector current correlator, Eq. (17). The mean and error have been obtained from a correlated fit in the range [3,21].

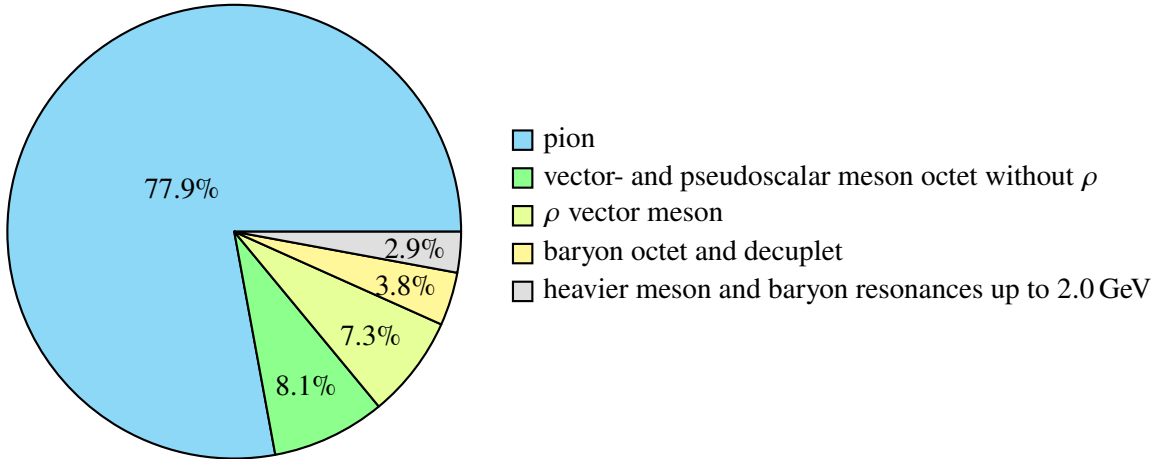


**Figure 4:** Relative composition of the total quark number susceptibility predicted by the hadron resonance gas model.

distributions, respectively. Resonances up to a mass of 2 GeV are included in the summation and we obtain  $\chi_q(T)/T^2 = 0.2428$  which is 5.8% above the aforementioned lattice estimate. By far the greatest contribution to the QNS is made by the pion (77.9%). The relative contributions of the remaining hadron species are visualized in Fig. 4. Sticking to the interpretation that collisions of pions with other hadrons are responsible for the modified dispersion relation, one could alternatively estimate the QNS taking only pions into account. However, one would then make use of the modified dispersion relation, Eq. (7) and integrate only up to a momentum cutoff  $\Lambda_p = 400$  MeV, where the chiral effective theory has been seen to break down in Ref. [3]. Employing this model we obtain

$\chi_q(T)/T^2 = 0.2163$  which is 5.3% below the lattice estimate. However, we would like to emphasize that this approach has little predictive power as it strongly depends on the momentum cutoff  $\Lambda_p$ .

## 5. Conclusion

On a  $(2 + 1)$ -flavor ensemble at physical quark masses we have seen that at a temperature  $T = 128$  MeV the thermal medium gives rise to a modified dispersion relation for the pion [see Eq. (7)]. The dispersion relation gets multiplied by a temperature dependent parameter  $u \approx 0.79$  which can be interpreted as the group velocity of a massless pion excitation in the chiral limit. Additionally, the pion velocity  $u$  links the screening pion mass  $m_\pi$  entering the modified dispersion relation to the quasiparticle mass  $\omega_0$ , which can be interpreted as the pole mass. While the screening mass increases relative to the zero-temperature pion mass when temperature is switched on, the quasi-particle mass decreases at the same time.

Furthermore, analyzing the difference  $(V - A)$  of temporal Euclidean two-point functions at zero and finite temperature, we conclude that chiral symmetry restoration is already at an advanced stage in terms of the spectral function. Finally, we have compared the quark number susceptibility  $\chi_q/T^2 = 0.2293(47)$  on the lattice to the hadron resonance gas model estimate which was 5.8% above the lattice estimate. By contrast to that, an approach where only the pion with its modified dispersion relation was taken into account results in an estimate which is 5.3% below the lattice estimate.

At the moment we are generating a thermal ensemble with the same parameters as the one analyzed here except for the time extent  $N_\tau = 20$  corresponding to a temperature  $T \approx 149$  MeV right below the chiral phase transition.

## Acknowledgments

This work was supported by the European Research Council (ERC) under the European Union's Horizon 2020 research and innovation program through Grant Agreement No. 771971-SIMDAMA, as well as by the Deutsche Forschungsgemeinschaft (DFG, German Research Foundation) through the Cluster of Excellence "Precision Physics, Fundamental Interactions and Structure of Matter" (PRISMA+ EXC 2118/1) funded by the DFG within the German Excellence strategy (Project ID 39083149). T.H. is supported by UK STFC CG ST/P000630/1. The generation of gauge configurations as well as the computation of correlators was performed on the Clover and Himster2 platforms at Helmholtz-Institut Mainz and on Mogon II at Johannes Gutenberg University Mainz. We made use of the following libraries: GNU Scientific Library [17], GNU MPFR [18] and GNU MP [19].

## References

- [1] R. Hagedorn, *How We Got to QCD Matter from the Hadron Side: 1984*, *Lect. Notes Phys.* **221** (1985) 53.
- [2] B.B. Brandt, A. Francis, H.B. Meyer and D. Robaina, *Chiral dynamics in the low-temperature phase of QCD*, *Phys. Rev. D* **90** (2014) 054509 [1406.5602].

- [3] B.B. Brandt, A. Francis, H.B. Meyer and D. Robaina, *Pion quasiparticle in the low-temperature phase of QCD*, *Phys. Rev. D* **92** (2015) 094510 [1506.05732].
- [4] M. Dey, V.L. Eletsky and B.L. Ioffe, *Mixing of vector and axial mesons at finite temperature: an Indication towards chiral symmetry restoration*, *Phys. Lett. B* **252** (1990) 620.
- [5] V.L. Eletsky and B.L. Ioffe, *On the current correlators in QCD at finite temperature*, *Phys. Rev. D* **47** (1993) 3083 [hep-ph/9302298].
- [6] V.L. Eletsky and B.L. Ioffe, *Next-to-leading order temperature corrections to correlators in QCD*, *Phys. Rev. D* **51** (1995) 2371 [hep-ph/9405371].
- [7] M. Cè, T. Harris, A. Krasniqi, H.B. Meyer and C. Török, *Aspects of chiral symmetry in QCD at  $T = 128$  MeV*, 2211.15558.
- [8] M. Bruno, T. Korzec and S. Schaefer, *Setting the scale for the CLS 2 + 1 flavor ensembles*, *Phys. Rev. D* **95** (2017) 074504 [1608.08900].
- [9] J. Bulava and S. Schaefer, *Improvement of  $N_f = 3$  lattice QCD with Wilson fermions and tree-level improved gauge action*, *Nucl. Phys. B* **874** (2013) 188 [1304.7093].
- [10] M. Lüscher and S. Schaefer, *Lattice QCD with open boundary conditions and twisted-mass reweighting*, *Comput. Phys. Commun.* **184** (2013) 519 [1206.2809].
- [11] M. Bruno et al., *Simulation of QCD with  $N_f = 2 + 1$  flavors of non-perturbatively improved Wilson fermions*, *JHEP* **02** (2015) 043 [1411.3982].
- [12] M. Cè et al., *Window observable for the hadronic vacuum polarization contribution to the muon  $g - 2$  from lattice QCD*, 2206.06582.
- [13] D.T. Son and M.A. Stephanov, *Pion propagation near the QCD chiral phase transition*, *Phys. Rev. Lett.* **88** (2002) 202302 [hep-ph/0111100].
- [14] D.T. Son and M.A. Stephanov, *Real time pion propagation in finite temperature QCD*, *Phys. Rev. D* **66** (2002) 076011 [hep-ph/0204226].
- [15] H.B. Meyer, *The bulk channel in thermal gauge theories*, *JHEP* **04** (2010) 099 (2010) [arXiv:1002.3343].
- [16] A. Gérardin, T. Harris and H.B. Meyer, *Nonperturbative renormalization and  $O(a)$ -improvement of the nonsinglet vector current with  $N_f = 2 + 1$  Wilson fermions and tree-level Symanzik improved gauge action*, *Phys. Rev. D* **99** (2019) 014519 [1811.08209].
- [17] M.G. et al. <https://gmplib.org/>, 2019.
- [18] L. Fousse, G. Hanrot, V. Lefèvre, P. Pélissier and P. Zimmermann, *Mpfr: A multiple-precision binary floating-point library with correct rounding*, *ACM Trans. Math. Softw.* **33** (2007) 13–es.
- [19] T. Granlund and the GMP development team. <https://gmplib.org/>, 2020.